ACS OMEGA

http://pubs.acs.org/journal/acsodf

Article

On the Importance of Noncovalent Interactions in the Stabilization of Nonconventional Compounds Using Bulky Groups

Rodrigo Báez-Grez and Ricardo Pino-Rios*

Cite This: *ACS Omega* 2023, 8, 23168−23173

Read Online

ACCESS | Metrics & More | Article Recommendations | Supporting Information

ABSTRACT: In this article, we studied the capability of bulky groups to contribute to the stabilization of a given compound in addition to the well-known steric effect related to substituents due to their composition (alkyl chains and aromatic groups, among others). For this purpose, the recently synthesized 1-bora-3-boratabenzene anion which contains large substituents was analyzed by means of the independent gradient model (IGM), natural population analysis (NPA) at the TPSS/def2-TZVP level, force field-based energy decomposition analysis (EDA-FF) applying the universal force field (UFF), and molecular dynamics calculations under the GFN2-xTB approach. The results indicate that the bulky groups should not only be considered for their steric effects but also for their ability to stabilize a system that could be very reactive.

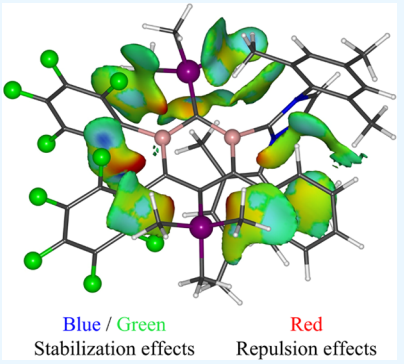

INTRODUCTION

In synthetic chemistry, the use of protecting groups is a very important and useful strategy that allows not only, as the name suggests, to protect a reactive area but also to stabilize unconventional chemical structures.[1−6] It is necessary to emphasize that the concept of stability we use goes not only beyond the thermodynamic stability studied in chemistry but also to the idea of stability used in material science or drug design, where it refers to compounds that are particularly nonreactive at certain conditions, such as temperature and pressure, among others.[7,8]

An important feature of the protective groups is their bulkiness;[9] these groups are often used as masking agents by preventing the interaction of highly reactive compounds.[10−15] Protection is usually attributed to steric effects mainly because they are usually composed of branched alkyls and/or aromatic rings. The use of these groups has led to the successful synthesis of different organic and inorganic compounds,[10−15] as well as those beyond these two fields of chemistry.[15−20] A clear example that became relevant in recent years is the synthesis of Zintl-type clusters, these structures contain both transition metals and main group compounds. In addition, they tend to be highly charged and reactive; however, the use of bulky groups enables the study of these compounds comprehensively.[21−23]

Another interesting area where the use of bulky groups has been applied is the synthesis of inorganic analogues of benzene and other aromatic systems.[24−33] Power's group has pioneered the synthesis of heavy analogues of benzene using mesityl, diisopropylphenyl, and other groups to stabilize the inorganic rings.[34] More recently, Seitz et al.[32] reported the synthesis of pnictogen−silicon benzene analogues, which possess a reasonable degree of aromaticity[35] and bulky protecting groups, such as tert-butyl, phenyl, and others, thus stabilizing the ring. On the other hand, in 2018, Heider et al.[36] synthesized a three-membered cyclic phosphasilene containing triisopropylphenyl groups, NHC (1,3-diisopropyl-4,5-dimethylimidazol-2-ylidene).

More recently, benzene analogues containing boron have been successfully synthesized. In 2020, the 9-borataphenanthrene anion has been prepared.[37] This compound is not only isoelectronic to phenanthrene but also possesses a similar aromatic character according to theoretical studies based on different criteria, such as magnetic, delocalization, and geometrical among others.[38] Recently, Sun et al.[39] synthesized the 1-bora-3-boratabenzene anion obtaining high yields. The substituents of this compound are phenyl, C_6F_5, $Si(CH_3)_3$, and *N*,*N*−dimesitylimidazolylidene, which, due to their large size (see Scheme 1), could help the stabilization of the anion. The aromaticity degree of boratabenzene has been proven by the authors through the magnetic criteria.

Bulky groups make use of the steric repulsion effect to prevent the reaction of the compounds of interest. However, we have the following questions: Is this the only effect that these substituents have? Is it possible that there are other

Received: April 18, 2023
Accepted: June 1, 2023
Published: June 13, 2023

https://doi.org/10.1021/acsomega.3c02663
ACS Omega 2023, 8, 23168−23173

Scheme 1. 2D Representation of the 1-Bora-3-boratabenzene Anion

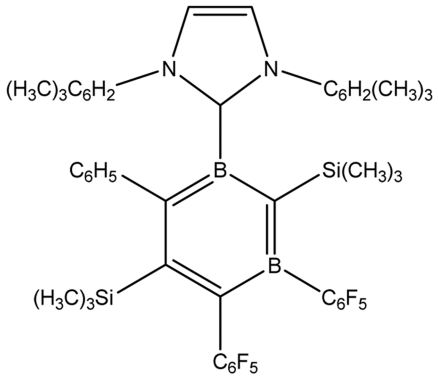

interactions that could help the stabilization of various unconventional systems? If so, how strong and/or stable are they? To answer these questions, we studied the topology and the dynamical behavior of the bulky substituted 1-bora-3-boratabenzene anion using the independent gradient model (IGM)[40] to understand the nature of the intramolecular interactions (see the Computational Methods section) in conjunction with an analysis of the kinetic stability by means of molecular dynamics simulations using the GFN2-xTB approach proposed by Grimme.[41] This method allows the study of large systems with a reasonable computational cost and very good results, especially in geometry prediction. The evaluation of root-mean-square deviation over time will allow us to understand the motion of the substituents and the average IGM (or aIGM) method, which is an extension of the method that allows the study of the flow of interactions from the molecular dynamics' trajectories. This will help us to understand the nature of stability between substituent interactions.

COMPUTATIONAL DETAILS

Cartesian coordinates of the 1-bora-3-boratabenzene anion were taken from the work of Sun et al.,[39] and a single point calculation was performed using the Gaussian 16 B.01[42] software package at the TPSS[43]/def2-TZVP[44] level has been carried out (see cartesian coordinates of the optimized system, Table S1). Independent gradient model (IGM) and average IGM calculations have been performed using the Multiwfn program.[45] IGM is based on the function g^{IGM}, which is analogous to the reduced density gradient ($s(r)$) used in NCI analysis,[46] i.e., it reveals zones where there would be weak interactions and like NCI uses the function $\text{sign}(\lambda_2)\rho(r)$ to identify the type of interaction. Thus, it is possible to identify hydrogen bonds, van der Waals interactions, and repulsive effects related to steric hindrance for negative, near zero, and positive values of $\text{sign}(\lambda_2)\rho(r)$, respectively. In addition, IGM offers certain advantages over NCI, first of all, it only needs the structure of the compound and the g^{IGM} function, it is smoother than $s(r)$ so the computational cost is reduced. The interpretation of IGM results is similar to those obtained through the popular NCI index. The blue regions are related to strong noncovalent interactions, such as hydrogen bonds (see the Results and Discussion section), while the red regions represent repulsive regions due to steric (Pauli) effects. On the other hand, the green regions are related to van der Waals type interactions. Another major advantage of IGM is that it is possible to decompose the g^{IGM} function into two or more fragments.[47] Regarding aIGM, this method needs the trajectories obtained from molecular dynamics simulations and to calculate the average electron density using promolecular approximation.[46,48,49] For this work, six fragments have been used, which represent each of the substituents of the aromatic ring, and the intramolecular interactions between them are studied.

Additionally, natural population analysis has been carried out for all of the substituents using the NBO 6.0 program.[50] To numerically evaluate the effects of electrostatic and dispersion interactions between fragments, energy decomposition analysis based on force fields implemented in Multiwfn has been performed.[51] An interesting feature of this analysis is that it allows a decomposition of more than two fragments making it ideal for our study. The universal force field (UFF)[52] has been used since we have B and Si atoms and also a smoothed $1/r^2$ function for the calculation of van der Waals (dispersion) contributions.

On the other hand, MD simulations have been performed using the GFN2-xTB Hamiltonian[41,53] for 50 ps. During the simulations, the equations of motion were integrated with a 1.0 fs time step in the constant number of atoms, constant volume, and constant temperature (NVT) ensemble at 100 K using a Berendsen thermostat to maintain this constant temperature. The SHAKE algorithm was applied for all hydrogen atoms.[54] Data were collected every 1 fs. For molecular visualization of the systems and MD trajectory analysis, the VMD program was used.[55] From the 50,000 structures obtained from the MD simulations, 2000 were taken using a delta of 25 frames for the IGM calculations. In addition, the thermal fluctuation index has been obtained in order to understand the stability of the intramolecular interactions over time. Visualization of the IGM analysis was performed with Chemcraft software.[56]

RESULTS AND DISCUSSION

Figure 1 shows the optimized structure of the 1-bora-3-boratabenzene anion at the TPSS/def2-TZVP level and the

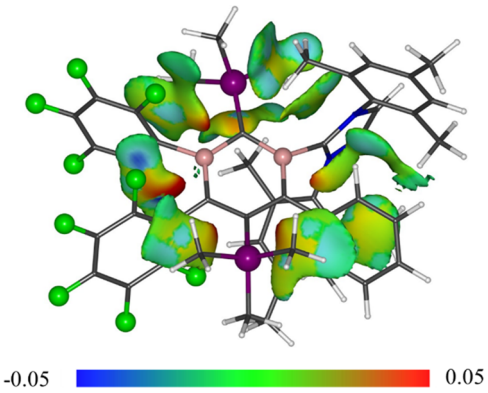

Figure 1. Independent gradient model results (in a.u.) for the 1-bora-3-boratabenzene anion at the TPSS/def2-TZVP level. Dark gray: carbon, white: hydrogen, purple: silicon, green: fluorine atoms.

isosurfaces, which represent the intramolecular interactions between the respective substituents. For the case of $-C_6F_5$, it is possible to observe weakly attractive (green) zones related to π-stacking between the aromatic rings. Additionally, a blue zone is observed between the fluorine atoms, which is distinctive for strong noncovalent interactions. This can be

https://doi.org/10.1021/acsomega.3c02663
ACS Omega 2023, 8, 23168−23173

attributed to the σ-hole[57] in fluorine atoms which, due to the position of the atoms, leads to stabilizing interactions. Additionally, a π-stacking interaction is observed between the displaced C_6H_5 substituents of the boratabenzene ring and the *N*,*N*-dimesitylimidazolylidene substituent. The interactions between alkyl substituents are van der Waals (vdW) type as well as those with the aromatic rings, which are π-alkyl vdW-type. These interactions have been observed in biological systems and are of great importance in the stabilization of ligand−protein complexes.[58]

On the other hand, Figure 2 shows the results of the population analysis in the context of NBO of the ring

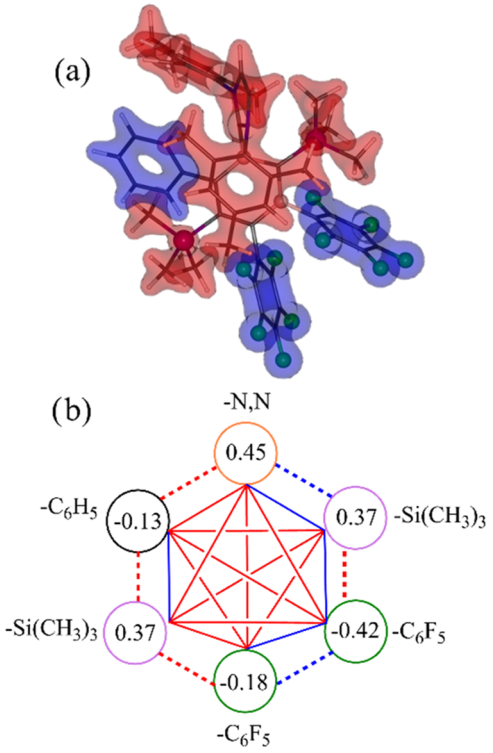

Figure 2. (a) Fragment NPA populations. Blue (red) color represents negative (positive) charges. (b) Numerical values of calculated fragment charges and lines representing attractive (red) and repulsive (blue) interactions. Dashed lines denote electrostatic interactions resulting from the charges, while solid lines represent the interactions obtained through the EDA-FF approach.

fragments. The total charges of the fragments can be seen in Figure 4a, the blue color represents that the total charge of the substituent is negative, while the red ones are positive. The values in Figure 4b represent the numerical values of the fragment charges as well as the dashed lines show whether the electrostatic interaction is attractive (red) or repulsive (blue). The values and dashed lines show that there are mostly attractive interactions. The repulsive interactions are between the larger fragment corresponding to the *N*,*N*-dimesitylimidazolylidene substituent and the nearby $Si(CH_3)_3$ substituent. The other repulsive interaction corresponds to that between the C_6F_5 substituents due to the total negative charge of each fragment.

Additionally, the EDA-FF results indicate that the overall interactions between the substituents are mostly attractive (solid red lines), while the repulsive interactions (solid blue lines) occur only between adjacent fragments. It is possible to note that the interactions are not only important between the fragments in close proximity but also those farther apart. In these cases, dispersion effects play a very important role, being the main contributor to the attractive interactions (see Table S2 in the SI). The results obtained are similar to those obtained by Cummins and co-workers,[59] who, through calculations based on the DPLNO-CCSD(T) method, reached the same conclusions. Fragment charges and EDA-FF values are in agreement with IGM visual analysis.

The results show that the attractive intramolecular interactions between bulky groups are not only useful to protect a ring or a desired molecular system but also help to stabilize the system due to their attractive nature; however, how persistent are these interactions?

To answer the above question, we have carried out a 50 ps molecular dynamics simulation at 1000 K of the 1-bora-3-boratabenzene anion, and the trajectory can be seen in the Supporting Information. First, it is necessary to point out that during the simulation, the boratabenzene ring persists in time, however, planarity is lost. Figure 3 shows the evolution of the

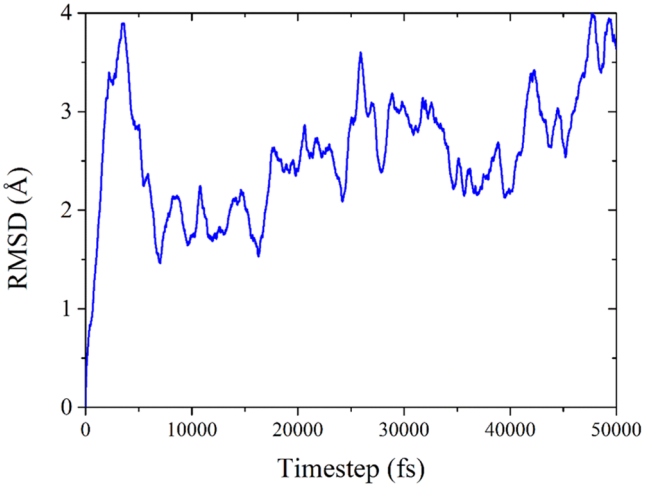

Figure 3. RMSD results (in Å) from trajectories (in fs) of the molecular dynamics simulations.

molecular motion in terms of the root-mean-square deviation (RMSD), the values are high, with an average of 2.57 Å; and a maximum value of 4.02 Å;, this should not be surprising due to the large number of degrees of freedom that the system has, especially for those substituents containing branched alkyl substituents. However, it is emphasized that large molecular motion does not mean that the system is unstable; however, it is clear that many of the intramolecular interactions are formed/broken due to the movement caused by the high temperature.

To evaluate the interactions over time, aIGM analysis was carried out by taking 2000 structures from the 50,000 obtained in molecular dynamics with a step size of 25 fs in order to cover the whole process at a reasonable computational cost. In addition, one structure was obtained based on the average of the atomic positions.

Figure 4 shows the aIGM results at the top. It is possible to observe that the interactions between π electrons in rings and the σ holes in halogens persist. Additionally, the van der Waals type interactions between the methyl groups also persist, however, there are red zones, related to Pauli repulsion, which

https://doi.org/10.1021/acsomega.3c02663
ACS Omega 2023, 8, 23168−23173

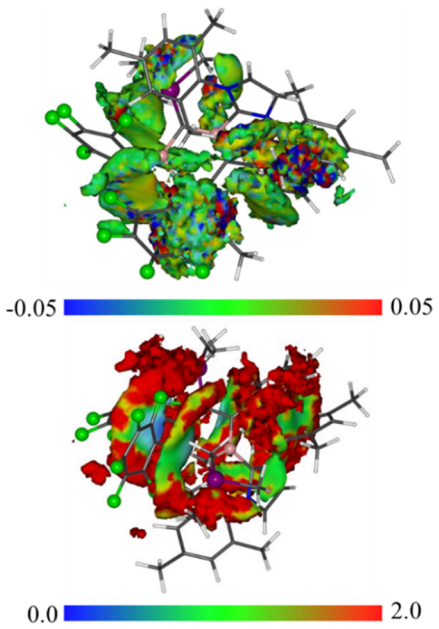

Figure 4. aIGM (top) and thermal fluctuation index (bottom) for average structure of the 1-bora-3-boratabenzene anion obtained from molecular dynamics simulations. Results in a.u.

appear due to the movement of the substituents, however, the attractive interactions are best observed.

On the other hand, we have calculated the thermal fluctuation index ($f(r)$) to evaluate the strength (stability) of the interactions due to molecular motion. In the bottom of Figure 4, one can observe red colored zones, which are related to high values of $f(r)$ and weak stability of the interactions, while the blue zones indicate very stable interactions, the green color is understood as structures with intermediate stability. In general, the interactions are mostly between unstable and moderately stable. One highly stable interaction is observed between the fluorinated rings and another between $-Si(CH_3)_3$ and a fluorinated ring. Additionally, π-stacking interactions between the phenyls are preserved. However, it is observed that the van der Waals interactions between the methyl groups are weak since red zones are shown. This is an indication that the attractive interactions are forming and breaking as time goes by, however, they are always there to support the stabilization of the molecule.

CONCLUSIONS

In the present study, we have evaluated the intramolecular interactions between bulky substituent groups in the stabilization of unconventional chemical species, going beyond the already known protective capacity of different species, through calculations of scalar functions derived from the electron density at the DFT level, natural population analysis, force field-based energy decomposition analysis, and molecular dynamics at high temperatures using the GNF2-xTB approach, as well as the use of the promolecular approximation of the electron density for the study of temporal changes. The results show that the π-stacking interactions of the fluorinated rings as well as between the σ holes are the strongest in the 1-bora-3-boratabenzene anion complex. Additionally, there are π-stacking interactions on the phenyl substituent and the aromatic rings found in *N*,*N*-dimesitylimidazolylidene. There are also interactions between the alkyls and aromatic rings. Results show attractive electrostatic interactions; however, the strongest attractive contributions are due to dispersion effects according to the results of the energy decomposition and NBO fragment population analysis shown.

These interactions have been evaluated over time using the aIGM method and the thermal fluctuation index. Although the alkyl−phenyl and alkyl−alkyl interactions are weak, as can be seen in the high RMSD values, they form and break down over time, while the π-stacking and σ-hole interactions are preserved in a medium to high degree and are thus very important in the stabilization of the complex. The presented results allow us to say that bulky groups should not only be treated as protectors of chemical species but also as stabilizing factors. This study intends to vindicate the intramolecular interactions between bulky groups as an alternative criterion in the synthesis of new chemical species.

ASSOCIATED CONTENT

Supporting Information

The Supporting Information is available free of charge at https://pubs.acs.org/doi/10.1021/acsomega.3c02663.

Molecular dynamics simulations (MP4)

Molecular dynamics simulation at 1000 K of 1-bora-3-boratabenzene anion and EDA force field results and cartesian coordinates (PDF)

AUTHOR INFORMATION

Corresponding Author

Ricardo Pino-Rios − *Química y Farmacia, Facultad de Ciencias de la Salud, Universidad Arturo Prat., Iquique 1100000, Chile;* orcid.org/0000-0003-4756-1115; Email: rpinorios@unap.cl

Author

Rodrigo Báez-Grez − *Computational and Theoretical Chemistry Group, Departamento de Ciencias Químicas, Facultad de Ciencias Exactas, Universidad Andres Bello, 8370146 Santiago, Chile;* orcid.org/0000-0001-9303-1559

Complete contact information is available at: https://pubs.acs.org/10.1021/acsomega.3c02663

Author Contributions

R.B.-G.: methodology, investigation, formal analysis; R.P.-R.: conceptualization, methodology, investigation, formal analysis.

Notes

The authors declare no competing financial interest.

ACKNOWLEDGMENTS

The authors thank the financial support of the National Agency for Research and Development (ANID) through FONDECYT Projects 1230571 (R.P.-R.) and FONDECYT Postdoctorado 3210037 (R.B.G.). Powered@NLHPC: this research was partially supported by the supercomputing infrastructure of the NLHPC (ECM−02) of the Universidad de Chile.

REFERENCES

(1) Vala, R. M.; Patel, D. M.; Sharma, M. G.; Patel, H. M. Impact of an Aryl Bulky Group on a One-Pot Reaction of Aldehyde with Malononitrile and N-Substituted 2-Cyanoacetamide. *RSC Adv.* **2019**, *9*, 28886−28893.

(2) Solomons, T. W. G.; Fryhle, C. B.; Snyder, S. A. *Organic Chemistry*; Wiley, 2016.
(3) Dagonneau, M.; Ivanov, V. B.; Rozantsev, E. G.; Sholle, V. D.; Kagan, E. S. Sterically Hindered Amines and Nitroxyls as Polymer Stabilizers. *J. Macromol. Sci., Part C* **1982**, *22*, 169−202.
(4) Errede, L. A.; McBrady, J. J.; Oien, H. T. Acylanthranils. 4. The Effect of Steric Hindrance on Selectivity in the Reaction of Amines with Acetylanthranil. *J. Org. Chem.* **1977**, *42*, 656−658.
(5) Brown, H. C. For an Early Account of the Effect of the Steric Hindrance on Chemical Reactivity *J. Chem. Soc.* 1956; Vol. *1248*.
(6) Sharma, M. G.; Rajani, D. P.; Patel, H. M. Green Approach for Synthesis of Bioactive Hantzsch 1,4-Dihydropyridine Derivatives Based on Thiophene Moiety via Multicomponent Reaction. *R. Soc. Open Sci.* **2022**, *4*, No. 170006.
(7) Triggle, D. J.; Taylor, J. B. *Comprehensive Medicinal Chemistry II*; Elsevier Science, 2006.
(8) Hussain, G.; Asghar, M.; Waqas Iqbal, M.; Ullah, H.; Autieri, C. Exploring the Structural Stability, Electronic and Thermal Attributes of Synthetic 2D Materials and Their Heterostructures. *Appl. Surf. Sci.* **2022**, *590*, No. 153131.
(9) Yadav, V. K. *Steric and Stereoelectronic Effects in Organic Chemistry*; Springer Singapore: Singapore, 2016.
(10) Shoji, Y.; Matsuo, T.; Hashizume, D.; Fueno, H.; Tanaka, K.; Tamao, K. A Stable Doubly Hydrogen-Bridged Butterfly-Shaped Diborane(4) Compound. *J. Am. Chem. Soc.* **2010**, *132*, 8258−8260.
(11) Li, B.; Matsuo, T.; Hashizume, D.; Fueno, H.; Tanaka, K.; Tamao, K. π-Conjugated Phosphasilenes Stabilized by Fused-Ring Bulky Groups. *J. Am. Chem. Soc.* **2009**, *131*, 13222−13223.
(12) Murosaki, T.; Kaneda, S.; Maruhashi, R.; Sadamori, K.; Shoji, Y.; Tamao, K.; Hashizume, D.; Hayakawa, N.; Matsuo, T. Synthesis and Structural Characteristics of Discrete Organoboron and Organoaluminum Hydrides Incorporating Bulky Eind Groups. *Organometallics* **2016**, *35*, 3397−3405.
(13) Kanazawa, S.; Ohira, T.; Goda, S.; Hayakawa, N.; Tanikawa, T.; Hashizume, D.; Ishida, Y.; Kawaguchi, H.; Matsuo, T. Synthesis and Structural Characterization of Lithium and Titanium Complexes Bearing a Bulky Aryloxide Ligand Based on a Rigid Fused-Ring s-Hydrindacene Skeleton. *Inorg. Chem.* **2016**, *55*, 6643−6652.
(14) Szilvási, T.; Veszprémi, T. Molecular Tailoring: Reaction Path Control with Bulky Substituents. *Organometallics* **2012**, *31*, 3207−3212.
(15) Shoji, Y.; Tanaka, N.; Mikami, K.; Uchiyama, M.; Fukushima, T. A Two-Coordinate Boron Cation Featuring C−B+−C Bonding. *Nat. Chem.* **2014**, *6*, 498−503.
(16) Chou, S.-L.; Lo, J.-I.; Peng, Y.-C.; Lin, M.-Y.; Lu, H.-C.; Cheng, B.-M.; Ogilvie, J. F. Identification of Diborane(4) with Bridging B−H−B Bonds. *Chem. Sci.* **2015**, *6*, 6872−6877.
(17) Agou, T.; Nagata, K.; Tokitoh, N. Synthesis of a Dialumene-Benzene Adduct and Its Reactivity as a Synthetic Equivalent of a Dialumene. *Angew. Chem., Int. Ed.* **2013**, *52*, 10818−10821.
(18) Pan, C.; Tang, G.; Cao, Z.; Xu, J.; Sheng, S. Structural and Theoretical Studies of a New CuI-CuI Complex Bearing Bulky Unsymmetrical Benzamidinate Ligand. *Chem. Res. Chin. Univ.* **2015**, *31*, 112−116.
(19) Jones, C.; Schulten, C.; Fohlmeister, L.; Stasch, A.; Murray, K. S.; Moubaraki, B.; Kohl, S.; Ertem, M. Z.; Gagliardi, L.; Cramer, C. J. Bulky Guanidinato Nickel(I) Complexes: Synthesis, Characterization, Isomerization, and Reactivity Studies. *Chem. - Eur. J.* **2011**, *17*, 1294−1303.
(20) Escomel, L.; Soulé, N.; Robin, E.; Del Rosal, I.; Maron, L.; Jeanneau, E.; Thieuleux, C.; Camp, C. Rational Preparation of Well-Defined Multinuclear Iridium−Aluminum Polyhydride Clusters and Comparative Reactivity. *Inorg. Chem.* **2022**, *61*, 5715−5730.
(21) Liu, C.; Sun, Z.-M. Recent Advances in Structural Chemistry of Group 14 Zintl Ions. *Coord. Chem. Rev.* **2019**, *382*, 32−56.
(22) Mondal, S.; Chen, W.-X.; Sun, Z.-M.; McGrady, J. E. Synthesis, Structure and Bonding in Pentagonal Bipyramidal Cluster Compounds Containing a Cyclo-Sn5 Ring, [(CO)3MSn5M(CO)3]4− (M = Cr, Mo). *Inorganics* **2022**, *10*, No. 75.
(23) Rienmüller, J.; Schmidt, A.; Yutronkie, N. J.; Clérac, R.; Werncke, C. G.; Weigend, F.; Dehnen, S. Reactive Solubilization of Heterometallic Clusters by Treatment of (TrBi3)2− Anions (Tr = Ga, In, Tl) with [Mn{N(SiMe3)2}2]. *Angew. Chem., Int. Ed.* **2022**, *61*, No. e202210683.
(24) Hu, Y. X.; Zhang, J.; Wang, X.; Lu, Z.; Zhang, F.; Yang, X.; Ma, Z.; Yin, J.; Xia, H.; Liu, S. H. One-Pot Syntheses of Irida-Polycyclic Aromatic Hydrocarbons. *Chem. Sci.* **2019**, *10*, 10894−10899.
(25) Hiroto, S. Heteroatoms in Bowl-Shaped Polycyclic Aromatic Hydrocarbons: Synthesis and Structures. *Chem. Lett.* **2021**, *50*, 1146−1155.
(26) Yapi, A. D.; Mustofa, M.; Valentin, A.; Chavignon, O.; Teulade, J.-C.; MALLIE, M.; Chapat, J.-P.; Blache, Y. New Potential Antimalarial Agents: Synthesis and Biological Activities of Original Diaza-Analogs of Phenanthrene. *Chem. Pharm. Bull.* **2000**, *48*, 1886−1889.
(27) Sergeeva, A. P.; Piazza, Z. A.; Romanescu, C.; Li, W.-L.; Boldyrev, A. I.; Wang, L.-S. B22− and B23−: All-Boron Analogues of Anthracene and Phenanthrene. *J. Am. Chem. Soc.* **2012**, *134*, 18065−18073.
(28) Karásek, P.; Planeta, J.; Roth, M. Aqueous Solubility Data for Pressurized Hot Water Extraction for Solid Heterocyclic Analogs of Anthracene, Phenanthrene and Fluorene. *J. Chromatogr. A* **2007**, *1140*, 195−204.
(29) Scheurle, P. I.; Mähringer, A.; Haug, T.; Biewald, A.; Axthammer, D.; Hartschuh, A.; Harms, L.; Wittstock, G.; Medina, D. D.; Bein, T. Helical Anthracene−Ethyne-Based MOF-74 Analogue. *Cryst. Growth Des.* **2022**, *22*, 2849−2853.
(30) Kirschbaum, T.; Rominger, F.; Mastalerz, M. An Isosteric Triaza Analogue of a Polycyclic Aromatic Hydrocarbon Monkey Saddle. *Chem. - Eur. J.* **2020**, *26*, 14560−14564.
(31) Chiavarino, B.; Crestoni, M. E.; Marzio, A. Di.; Fornarini, S.; Rosi, M. Gas-Phase Ion Chemistry of Borazine, an Inorganic Analogue of Benzene. *J. Am. Chem. Soc.* **1999**, *121*, 11204−11210.
(32) Seitz, A. E.; Eckhardt, M.; Erlebach, A.; Peresypkina, E. V.; Sierka, M.; Scheer, M. Pnictogen-Silicon Analogues of Benzene. *J. Am. Chem. Soc.* **2016**, *138*, 10433−10436.
(33) Barnard, J. H.; Brown, P. A.; Shuford, K. L.; Martin, C. D. 1,2-Phosphaborines: Hybrid Inorganic/Organic P−B Analogues of Benzene. *Angew. Chem., Int. Ed.* **2015**, *54*, 12083−12086.
(34) Ota, K.; Kinjo, R. Inorganic Benzene Valence Isomers. *Chem. - Asian J.* **2020**, *15*, 2558−2574.
(35) Pino-Rios, R.; Vásquez-Espinal, A.; Alvarez-Thon, L.; Tiznado, W. Relativistic Effects on the Aromaticity of E3M3H3 (E = C−Pb; M = N−Bi) Benzene Analogues. *Phys. Chem. Chem. Phys.* **2020**, *22*, 22973−22978.
(36) Heider, Y.; Willmes, P.; Mühlhausen, D.; Klemmer, L.; Zimmer, M.; Huch, V.; Scheschkewitz, D. A Three-Membered Cyclic Phosphasilene. *Angew. Chem.* **2018**, *131*, 1958−1964.
(37) Bartholome, T. A.; Kaur, A.; Wilson, D. J. D.; Dutton, J. L.; Martin, C. D. The 9-Borataphenanthrene Anion. *Angew. Chem., Int. Ed.* **2020**, *59*, 11470−11476.
(38) Báez-Grez, R.; Pino-Rios, R. Borataalkene or Boratabenzene? Understanding the Aromaticity of 9-Borataphenanthrene Anions and Its Central Ring. *New J. Chem.* **2020**, *44*, 18069−18073.
(39) Sun, Q.; Daniliuc, C. G.; Mück-Lichtenfeld, C.; Kehr, G.; Erker, G. Formation of a Hybrid 1-Bora-3-Boratabenzene Heteroarene Anion Derivative. *Angew. Chem., Int. Ed.* **2022**, *61*, No. e202217504.
(40) Lefebvre, C.; Khartabil, H.; Boisson, J.-C.; Contreras-García, J.; Piquemal, J.-P.; Hénon, E. The Independent Gradient Model: A New Approach for Probing Strong and Weak Interactions in Molecules from Wave Function Calculations. *ChemPhysChem* **2018**, *19*, 724−735.
(41) Bannwarth, C.; Ehlert, S.; Grimme, S. GFN2-XTB—An Accurate and Broadly Parametrized Self-Consistent Tight-Binding Quantum Chemical Method with Multipole Electrostatics and Density-Dependent Dispersion Contributions. *J. Chem. Theory Comput.* **2019**, *15*, 1652−1671.

https://doi.org/10.1021/acsomega.3c02663
ACS Omega 2023, 8, 23168−23173

(42) Frisch, M. J.; Trucks, G. W.; Schlegel, H. B.; Scuseria, G. E.; Robb, M. A.; Cheeseman, J. R.; Scalmani, G.; Barone, V.; Petersson, G. A.; Nakatsuji, H.et al. *Gaussian 16*, Revisión B.01; Gaussian, Inc.: Wallingford CT, 2016.
(43) Tao, J.; Perdew, J. P.; Staroverov, V. N.; Scuseria, G. E. Climbing the Density Functional Ladder: Nonempirical Meta–Generalized Gradient Approximation Designed for Molecules and Solids. *Phys. Rev. Lett.* **2003**, *91*, No. 146401.
(44) Weigend, F.; Ahlrichs, R. Balanced Basis Sets of Split Valence, Triple Zeta Valence and Quadruple Zeta Valence Quality for H to Rn: Design and Assessment of Accuracy. *Phys. Chem. Chem. Phys.* **2005**, *7*, 3297−3305.
(45) Lu, T.; Chen, F. Multiwfn: A Multifunctional Wavefunction Analyzer. *J. Comput. Chem.* **2012**, *33*, 580−592.
(46) Johnson, E. R.; Keinan, S.; Mori-Sánchez, P.; Contreras-García, J.; Cohen, A. J.; Yang, W. Revealing Noncovalent Interactions. *J. Am. Chem. Soc.* **2010**, *132*, 6498−6506.
(47) Ponce-Vargas, M.; Lefebvre, C.; Boisson, J.-C.; Hénon, E. Atomic Decomposition Scheme of Noncovalent Interactions Applied to Host−Guest Assemblies. *J. Chem. Inf. Model.* **2020**, *60*, 268−278.
(48) Amat, L.; Carbó-Dorca, R. Use of Promolecular ASA Density Functions as a General Algorithm to Obtain Starting MO in SCF Calculations. *Int. J. Quantum Chem.* **2002**, *87*, 59−67.
(49) Pendás, A. M.; Luaña, V.; Pueyo, L.; Francisco, E.; Mori-Sánchez, P. Hirshfeld Surfaces as Approximations to Interatomic Surfaces. *J. Chem. Phys.* **2002**, *117*, 1017−1023.
(50) Glendening, E. D.; Landis, C. R.; Weinhold, F. NBO 6.0: Natural Bond Orbital Analysis Program. *J. Comput. Chem.* **2013**, *34*, 1429−1437.
(51) Lu, T.; Liu, Z.; Chen, Q. Comment on "18 and 12 − Member Carbon Rings (Cyclo[n]Carbons) − A Density Functional Study.". *Mater. Sci. Eng. B* **2021**, *273*, No. 115425.
(52) Rappe, A. K.; Casewit, C. J.; Colwell, K. S.; Goddard, W. A. I. I. I.; Skiff, W. M. UFF, a Full Periodic Table Force Field for Molecular Mechanics and Molecular Dynamics Simulations. *J. Am. Chem. Soc.* **1992**, *114*, 10024−10035.
(53) Grimme, S.; Bannwarth, C.; Shushkov, P. A Robust and Accurate Tight-Binding Quantum Chemical Method for Structures, Vibrational Frequencies, and Noncovalent Interactions of Large Molecular Systems Parametrized for All Spd-Block Elements (Z = 1−86). *J. Chem. Theory Comput.* **2017**, *13*, 1989−2009.
(54) Ryckaert, J.-P.; Ciccotti, G.; Berendsen, H. J. C. Numerical Integration of the Cartesian Equations of Motion of a System with Constraints: Molecular Dynamics of n-Alkanes. *J. Comput. Phys.* **1977**, *23*, 327−341.
(55) Humphrey, W.; Dalke, A.; Schulten, K. VMD: Visual Molecular Dynamics. *J. Mol. Graphics* **1996**, *14*, 33−38.
(56) Chemcraft. Chemcraft. Graphical. https://www.chemcraftprog.com.
(57) Politzer, P.; Murray, J. S. σ-Hole Interactions: Perspectives and Misconceptions. *Crystals* **2017**, *7*, No. 212.
(58) DiStasio, R. A.; Von Lilienfeld, O. A.; Tkatchenko, A. Collective Many-Body van Der Waals Interactions in Molecular Systems. *Proc. Natl. Acad. Sci. U.S.A.* **2012**, *109*, 14791−14795.
(59) Riu, M.-L. Y.; Bistoni, G.; Cummins, C. C. Understanding the Nature and Properties of Hydrogen−Hydrogen Bonds: The Stability of a Bulky Phosphatetrahedrane as a Case Study. *J. Phys. Chem. A* **2021**, *125*, 6151−6157.

https://doi.org/10.1021/acsomega.3c02663
ACS Omega 2023, 8, 23168−23173